



1 **Measurement report: Characteristics of**  
2 **aminiums in PM<sub>2.5</sub> during winter clean and**  
3 **polluted episodes in China: aminium outbreak**  
4 **and its constraint**

5

6

7 Yu Xu<sup>1</sup>, Tang Liu<sup>1</sup>, Yi-Jia Ma<sup>1</sup>, Qi-Bin Sun<sup>2</sup>, Hong-Wei Xiao<sup>1</sup>, Hao Xiao<sup>1</sup>, Hua-Yun

8 Xiao<sup>1,\*</sup>

9

10 <sup>1</sup>School of Agriculture and Biology, Shanghai Jiao Tong University, Shanghai 200240,

11 China

12 <sup>2</sup>Dongguan Meteorological Bureau, Dongguan, Guangdong, 523086, China

13

14

15

16

17

\*Corresponding authors

18

Hua-Yun Xiao

19

E-mail: xiaohuayun@sjtu.edu.cn

20

21

22



23 **Abstract:** Amines and aminiums play an important role in particle formation, liquid-  
24 phase reactions, and climate change, attracting considerable attention over the years.  
25 Here, we investigated the concentrations and compositions of aminiums in PM<sub>2.5</sub> in  
26 11 Chinese cities during the winter, focusing on the characteristics of aminiums  
27 during the polluted days and the key factors influencing aminium outbreak.  
28 Monomethylaminium was the dominant aminium species in most cities excepting  
29 Taiyuan and Guangzhou, followed by dimethylaminium. Diethylaminium dominated  
30 the total aminiums in Taiyuan and Guangzhou. Thus, the main amine sources in  
31 Taiyuan and Guangzhou were significantly different from those in other cities. The  
32 concentrations of the total aminiums (TA) in all cities increased significantly during  
33 the polluted days, with weak aminium outbreaks in Xi'an and Beijing. Additionally,  
34 the concentrations of TA in Xi'an and Beijing were insignificantly correlated with  
35 those of PM<sub>2.5</sub> and the major acidic aerosol components, while the opposite pattern  
36 was observed in 9 other cities. Thus, acid-base chemistry was significantly associated  
37 with the formation of aminiums in PM<sub>2.5</sub> in all cities excepting Xi'an and Beijing.  
38 Based on the sensitivity analysis of the aminiums/ammonium ratio to ammonium  
39 changes as well as excluding the effects of relative humidity and atmospheric  
40 oxidation, we proposed the possibility of the competitive uptake of ammonia versus  
41 amines on acidic aerosols or the displacement of aminiums by ammonia in Xi'an and  
42 Beijing (constraining aminium outbreaks). Overall, this study deepens the  
43 understanding of the spatiotemporal differences in aminium characteristic and  
44 formation in China. However, the uptake of amines on particles to form aminiums and



45 the relevant influencing factors require further mechanistic research.

46

47 **Keywords:** Aminiums, PM<sub>2.5</sub> pollution, Aerosol acidity, Spatiotemporal variations,

48 Formation mechanism

49

50

## 51 **1. Introduction**

52 Low-molecular-weight amines are ubiquitous and important in the gaseous and  
53 particulate phases (Nielsen et al., 2012; Ge et al., 2011a; Berta et al., 2023). More  
54 than 150 amines have been identified in the atmosphere (Ge et al., 2011a). The most  
55 abundant and frequently reported amines in field observations are typically C1–C6  
56 alkylamines including dimethylamine, monomethylamine, trimethylamine,  
57 diethylamine, ethylamine, 1-propanamine, and 1-butanamine (Yang et al., 2023b; Liu  
58 et al., 2023). Amines can participate in various chemical and physical processes in the  
59 atmosphere, promoting the formation and growth of new particles and contributing to  
60 the production of secondary organic aerosols (Yao et al., 2018; Tong et al., 2020;  
61 Møller et al., 2020). Amines are thus considered to have a direct or indirect impact on  
62 air quality (Li et al., 2019; Tao et al., 2016; Shen et al., 2023). Air pollution (e.g.,  
63 haze) caused by high levels of atmospheric fine particles (PM<sub>2.5</sub>) has received  
64 considerable attention in China over the past decade due to rapid industrialization and  
65 urbanization (Liu et al., 2022b; Liu et al., 2022c). Evidently, controlling the emission  
66 strength of amine sources and understanding the transformation of atmospheric



67 amines can effectively reduce air pollution in cities.

68       The main sources of atmospheric amines during the air pollution period in cities  
69 in China are typically fossil fuel combustion and biomass burning rather than  
70 agricultural emissions (Feng et al., 2022; Liu et al., 2022c; Wang et al., 2022; Shen et  
71 al., 2017; Ho et al., 2016; Chang et al., 2022). Owing to the water solubility and  
72 alkalinity of amines, low-molecular-weight amines in PM<sub>2.5</sub> during the air pollution  
73 period are mainly present in the form of amine salts (i.e., aminiums) via the gas-to-  
74 particle partitioning of gaseous amines and subsequent acid-base chemistry (Zhang et  
75 al., 2021; Liu et al., 2022a; Ge et al., 2011a; Xie et al., 2018). It should be noted that  
76 organic amines (e.g., dimethylamine and trimethylamine) in nanoparticles (<200 nm)  
77 may also be largely present in the organic phase (Xie et al., 2018). In addition,  
78 oxidative degradation of higher-molecular-weight amines and displacement reactions  
79 are also potential formation pathways of aminiums in PM<sub>2.5</sub> (Tao et al., 2021; Qiu and  
80 Zhang, 2013; Tong et al., 2020). Although previous observational studies have  
81 investigated the compositions, concentrations, sources, and formation processes of  
82 low-molecular-weight aminiums in the particle phase in urban areas of Shanghai (Liu  
83 et al., 2023), Guangzhou (Shu et al., 2023), Qingdao (Liu et al., 2022c), Xuzhou  
84 (Yang et al., 2023b), China, there has been relatively little focus on the association  
85 between PM<sub>2.5</sub> and amine outbreaks. A recent study conducted in Wangdu County,  
86 Hebei Province, China has suggested that amines exhibited outbreak characteristics  
87 during the haze episode (Feng et al., 2022). Climate and air pollution conditions can  
88 vary greatly from city to city due to the vastness of China. However, it is poorly



89 understood how the characteristics and formation processes of low-molecular-weight  
90 aminiums in PM<sub>2.5</sub> vary between clean and polluted days in different cities in China,  
91 which may hinder the further assessment of the environmental impacts of amines with  
92 regional differences.

93 In winter in China, air pollution episodes are more frequent compared to other  
94 seasons. Thus, we present the measurements of aminiums in PM<sub>2.5</sub> collected from 11  
95 different Chinese cities during the winter (2017–2018). The aims of this study are (1)  
96 to investigate the spatial differences in the compositions and concentrations of  
97 aminiums in PM<sub>2.5</sub>, with a focus on the difference between them on clean days and  
98 polluted days, and (2) to understand the key factors controlling the formation of  
99 aminiums in PM<sub>2.5</sub> in different cities.

100

## 101 **2. Materials and Methods**

### 102 **2.1. Site Description and Sample Collection**

103 A total of eleven urban sites were selected for aerosol sample collection,  
104 including Beijing (BJ; 116.41°E, 40.04°N), Taiyuan (TY; 112.58°E, 37.80°N), Xi'an  
105 (XA; 108.98°E, 34.25°N), Lanzhou (LZ; 103.73°E, 36.11°N), Haerbin (HEB, i.e.,  
106 Harbin; 126.64°E, 45.77°N), Wulumuqi (WLMQ, i.e., Urumqi; 87.75°E, 43.86°N),  
107 Chengdu (CD; 104.14°E, 30.68°N), Guiyang (GY; 106.73°E, 26.58°N), Guangzhou  
108 (GZ; 113.35°E, 23.18°N), Wuhan (WH; 114.36°E, 30.55°N), and Hangzhou (HZ;  
109 120.16°E, 30.30°N) sites (**Figure S1**). HZ and GZ are megacities situated in the  
110 Yangtze River Delta (YRD) and Pearl River Delta (PRD) regions respectively, both of



111 which have developed economies. WH is located in the central region of China. CD  
112 and GY are representative cities in southwest China. LZ, XA, TY, BJ, and HEB are  
113 cities in northern China. WLMQ, located in northwest China, is the largest inland city  
114 farthest from the ocean in the world. Obviously, the varying geographical locations  
115 and economic development levels of different cities inevitably lead to different air  
116 pollution and climate conditions between them.

117  $PM_{2.5}$  sampling in most cities was conducted on the rooftops of buildings (4–6  
118 floors in total) using a high-volume air sampler (Series 2031, Laoying, China) from  
119 December 1, 2017 to January 21, 2018 (winter). The sampling campaign in WLMQ  
120 was performed from March 3–28, 2018. At each site,  $PM_{2.5}$  was sampled once every  
121 one to two days for ~24 hours on prebaked quartz fiber filters (500 °C for 8 hours);  
122 moreover, two random blank filters were collected. The total number of  $PM_{2.5}$   
123 samples at each sampling site was shown in **Tables S1-S3**. All samples were stored at  
124 –30 °C until analysis. Meteorological data such as precipitation, wind speed,  
125 temperature, and relative humidity (RH), as well as concentrations of various  
126 pollutants were recorded during the sampling campaigns from the adjacent  
127 environmental monitoring stations. Sampling periods were classified as either clean or  
128 polluted days based on a daily average  $PM_{2.5}$  mass concentration of  $75 \mu\text{g m}^{-3}$  (Zhang  
129 and Cao, 2015).

130

## 131 **2.2. Chemical Analysis**

132 The extraction of low-molecular-weight aminiums in the filter samples was



133 carried out using the method described in our recent publication (Liu et al., 2023) and  
134 in a previous study (Liu et al., 2017). Briefly, the sample was filtered using a 0.22  $\mu\text{m}$   
135 Teflon syringe filter (CNW Technologies GmbH) after extraction with Milli-Q water  
136 ( $\sim 18.2 \text{ M}\Omega \text{ cm}$ ). The aminiums in the extracts that underwent pH regulation were  
137 derivatized using 0.1 mL of benzenesulfonyl chloride (BSC). The tube containing the  
138 derivatives was sealed and agitated for 30 minutes. To remove excess derivatization  
139 reagents, the extracts were agitated again for 30 minutes at 80°C after adding NaOH  
140 solution (0.5 mL of 10 mol L<sup>-1</sup>). Once the mixed solution had cooled down, it was  
141 acidified with a solution of HCl to adjust the pH to 5.5. A further extraction of  
142 derivatives was carried out by adding dichloromethane. It is important to mention that  
143 the organic phase was treated with Na<sub>2</sub>CO<sub>3</sub> solution and anhydrous Na<sub>2</sub>SO<sub>4</sub>  
144 sequentially. A stream of nitrogen gas was used to concentrate the organic extracts.  
145 Finally, the sample was analyzed using GC-MS after adding dichloromethane and  
146 hexamethylbenzene. Dimethylaminium (DMAH<sup>+</sup>), monomethylaminium (MMAH<sup>+</sup>),  
147 diethylaminium (DEAH<sup>+</sup>), ethylaminium (EAH<sup>+</sup>), propylaminium (PAH<sup>+</sup>),  
148 butylaminium (BAH<sup>+</sup>), and pyrrolidinium (PYRH<sup>+</sup>) were quantified. Aminium  
149 recoveries varied between 73% for DMAH<sup>+</sup> and 112% for PAH<sup>+</sup>. The determination  
150 limits of the aminium measurements ranged from 0.8 ng mL<sup>-1</sup> for DEAH<sup>+</sup> to 2.8 ng  
151 mL<sup>-1</sup> for MMAH<sup>+</sup>. Aminiums are undetectable in the blank. Detailed data quality  
152 controls were described in our recent publication (Liu et al., 2023).

153 Another filter cut was extracted with Milli-Q water to measure the  
154 concentrations of inorganic ions (e.g., NO<sub>3</sub><sup>-</sup>, SO<sub>4</sub><sup>2-</sup>, NH<sub>4</sub><sup>+</sup>, K<sup>+</sup>, Na<sup>+</sup>, Ca<sup>2+</sup>, and Mg<sup>2+</sup>) and



155 organic acids (e.g., acetic acid, formic acid, succinic acid, oxalic acid, glutaric acid,  
156 and methanesulfonic acid) (Xu et al., 2022a; Xu et al., 2023; Liu et al., 2023; Lin et  
157 al., 2023). These inorganic ions were quantified via an ion chromatograph system  
158 (Dionex Aquion, Thermo Scientific, USA).

159

### 160 **2.3. Parameter calculation**

161 The thermodynamic model (ISORROPIA-II) was used for the prediction of the  
162 mass concentration of aerosol liquid water (ALW) and the pH value, which was  
163 detailed in our previous studies (Xu et al., 2022b; Xu et al., 2020; Xu et al., 2023).  
164 The ventilation coefficient (VC) can be used as an indicator to assess the state of  
165 atmospheric dilution of pollutant concentrations (Gani et al., 2019). It is calculated by  
166 multiplying the wind speed by the planetary boundary layer height (PBLH) (Yang et  
167 al., 2023a).

168

## 169 **3. Results and discussion**

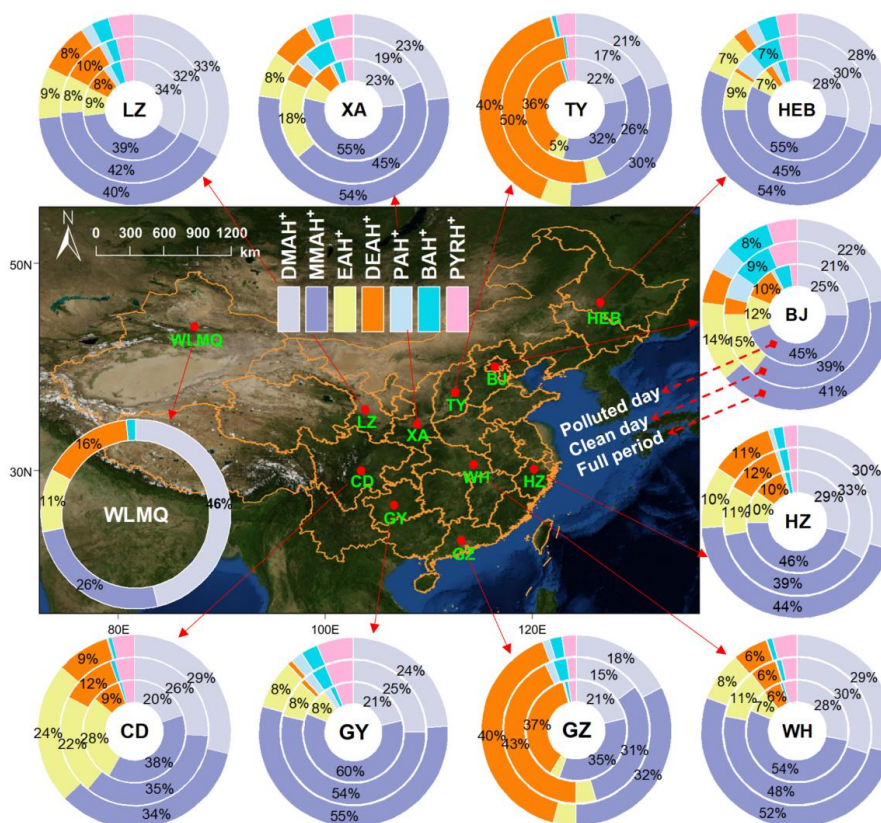
### 170 **3.1. Compositions of aminiums in PM<sub>2.5</sub> in China during winter**

171 **Figure 1** shows the average percentage distributions of various aminiums in  
172 PM<sub>2.5</sub> collected in different cities in China during winter, with a comparison between  
173 their mass fractions on clean and polluted days. MMAH<sup>+</sup> was the predominant species  
174 among the aminiums investigated in PM<sub>2.5</sub> in most cities in northern China, including  
175 LZ, XA, HEB, BJ, and WLMQ. MMAH<sup>+</sup>, along with the second most abundant  
176 DMAH<sup>+</sup>, accounted for more than 63% of the total aminium concentrations in those





177 northern cities; moreover, the relatively minor species, such as  $\text{DEAH}^+$ ,  $\text{EAH}^+$ ,  $\text{PAH}^+$ ,  
178  $\text{BAH}^+$ , and  $\text{PYRH}^+$ , contributed 1–18% of the total aminium concentrations,  
179 respectively. The predominance of  $\text{MMAH}^+$  was also found in cities in the YRD (HZ),  
180 central (WH), and southwestern (CD and GY) China, closely followed by  $\text{DMAH}^+$ .  
181 Previous studies conducted in Xi'an (winter, China) (Ho et al., 2015), Beijing (winter,  
182 China) (Wang et al., 2022; Ho et al., 2016), Nanjing (winter, China) (Liu et al., 2023)  
183 Shanghai (winter, China) (Liu et al., 2023), Xiamen (winter, China) (Ho et al., 2016),  
184 Hong Kong (winter, China) (Ho et al., 2016), and Arabian Sea (autumn and winter)  
185 (Gibb et al., 1999), as well as at mountain (autumn, Nanling, China) (Liu et al., 2018)  
186 and background (winter, Puding, China) (Liu et al., 2023) sites have suggested that  
187 the mass concentration fraction of  $\text{MMAH}^+$  was highest in the measured aerosol  
188 amine salts. The Henry's constants of MMA ( $3.65 \times 10^1 \text{ mol kg}^{-1} \text{ atm}^{-1}$ ), DMA ( $3.14$   
189  $\times 10^1 \text{ mol kg}^{-1} \text{ atm}^{-1}$ ), and EA ( $3.55 \times 10^1 \text{ mol kg}^{-1} \text{ atm}^{-1}$ ) are relatively lower than  
190 those of the other amines investigated (e.g.,  $1.32 \times 10^2 \text{ mol kg}^{-1} \text{ atm}^{-1}$  for DEA) (Ge  
191 et al., 2011b), implying that MMA, DMA, and EA are more easily partitioned into  
192 aqueous particles. Additionally, the gaseous forms of these determined aminiums  
193 typically have strong alkalinity (Ge et al., 2011b). This consideration combined with  
194 the increased emissions or weakened diffusions (lower PBLH on polluted days  
195 (**Tables S1-S3**)) of MMA and DMA may partially explain the high abundance of  
196  $\text{MMAH}^+$  and  $\text{DMAH}^+$  in  $\text{PM}_{2.5}$  in these investigated cities during winter.



197

198 **Figure 1.** Average percentage distributions of various aminiums in PM<sub>2.5</sub> collected in  
 199 different cities in China during winter. The map was obtained from ©MeteoInfoMap  
 200 (version 3.3.0) (Chinese Academy of Meteorological Sciences, China).

201

202 In another northern city (i.e., TY), DEAH<sup>+</sup> was the most abundant aminium  
 203 species (40% of the total aminium concentrations), followed by MMAH<sup>+</sup> (30%) and  
 204 DMAH<sup>+</sup> (21%). The composition characteristic of aminiums in the city of GZ (PRD  
 205 area) was similar to that observed in TY (**Figure 1**). Anthropogenic emissions,  
 206 including vehicle exhaust and industrial production are considered to be the main  
 207 contributors to aerosol DEAH<sup>+</sup> in urban areas (Chen et al., 2022b; Chen et al., 2019;



208 Yang et al., 2023b; Chang et al., 2022). In addition, previous studies have suggested  
209 that aerosol  $\text{DEAH}^+$  can also be largely derived from marine emissions (Facchini et  
210 al., 2008; Dall’osto et al., 2019). Thus, the relative emission strength of anthropogenic  
211 DEA in the investigated amines was probably higher in TY (the inland city) than in  
212 other cities. Since GZ is a developed coastal city, local aerosol aminiums may be  
213 influenced by large gaseous DEA inputs from both local industrial production and  
214 marine sources.

215 The mass concentration fractions of aminiums on clean and polluted days were  
216 also compared (**Figure 1**). The dominant aminium species (i.e.,  $\text{MMAH}^+$ ,  $\text{DMAH}^+$ , or  
217  $\text{DEAH}^+$ ) in  $\text{PM}_{2.5}$  in all cities were not replaced by other aminiums from the clean  
218 days to the polluted days. This likely suggests that the main sources of atmospheric  
219 gas-phase amines in the cities did not change significantly on the polluted days. In  
220 addition, the proportions of  $\text{MMAH}^+$  and  $\text{DMAH}^+$  tended to further increase from the  
221 clean days to the polluted days, while that of  $\text{DEAH}^+$  with relatively low solubility  
222 showed a decreasing trend, especially in TY and GZ (where  $\text{DEAH}^+$  was dominant).  
223 The concentrations of ALW in  $\text{PM}_{2.5}$  were generally much higher on polluted days  
224 than on clean days, especially in the northern cities (**Tables S1-S3**). Clearly, liquid-  
225 phase processes likely played an important role in the formation of aminiums on  
226 polluted days.

227

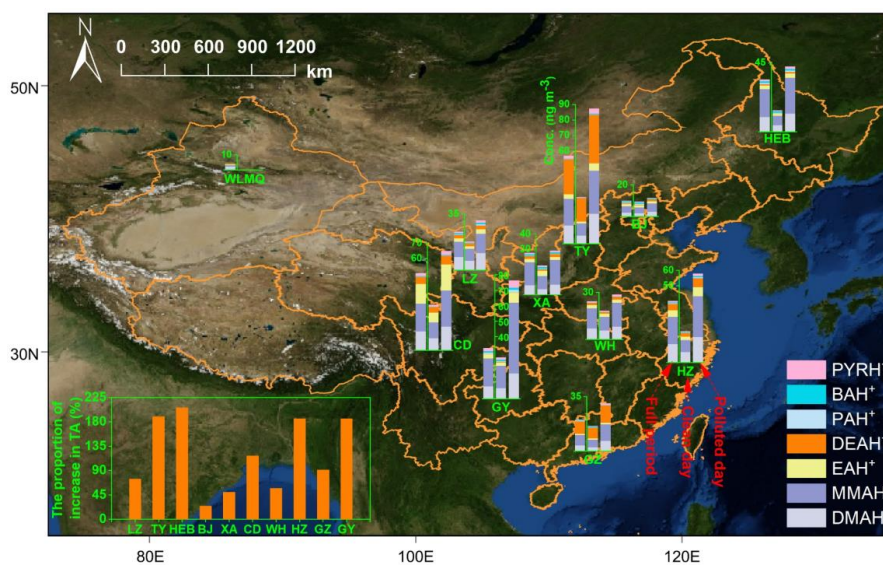
### 228 **3.2. Aminium concentrations and their linkage with $\text{PM}_{2.5}$ variations**

229 **Figure 2** shows the average concentration distributions of various aminiums in



230 PM<sub>2.5</sub> collected in different cities in China during winter, focusing on the difference  
 231 between their concentrations on clean days and polluted days. The concentrations of  
 232 total aminiums (TA) in TY ranged from 17.5 to 149.0 ng m<sup>-3</sup>, with an average of  
 233 56.90 ± 41.81 ng m<sup>-3</sup>. This average TA level was the highest among all the cities  
 234 investigated. The average concentration of TA in WLMQ was found to be the lowest  
 235 (4.16 ± 1.24 ng m<sup>-3</sup>), with a range of 2.10–6.50 ng m<sup>-3</sup>. As previously mentioned,  
 236 WLMQ is a vast city with a lower population density and less developed industries  
 237 compared to the more developed northern and coastal cities in China; moreover, the  
 238 region is surrounded by barren mountains and sandy land (Ma et al., 2024) (**Figure**  
 239 **2**). This appears to be responsible for the low levels of aminiums in the WLMQ.

240



241

242 **Figure 2.** Average concentration distributions of various aminiums in PM<sub>2.5</sub> collected  
 243 in different cities in the winter in China. The stacked bar chart from left to right  
 244 indicates the data for the full sampling period, the clean day, and the polluted day in



245 turn. The column chart in the bottom left corner shows the proportion of the increase  
246 in TA concentration from the clean days to the polluted days. The map was obtained  
247 from <sup>©</sup>MeteoInfoMap (version 3.3.0) (Chinese Academy of Meteorological Sciences,  
248 China).

249

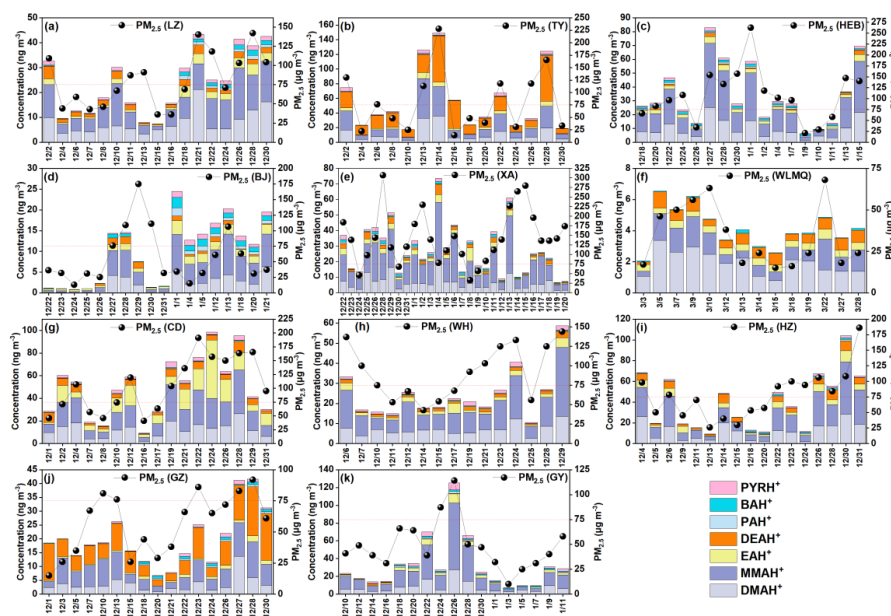
250 **Table S4** provides an overview of the aminiums detected in atmospheric fine  
251 particles detected in different seasons and regions. The ranges of average TA  
252 concentrations in the northern cities (i.e., HEB, BJ, TY, XA, LZ, and WLMQ)  
253 generally overlapped with those measured in the coastal (GZ and HZ), central (WH),  
254 and southwestern (CD and GY) cities in this study (**Tables S1-S3**) and were also  
255 comparable to the observation ranges reported in previous studies (Ho et al., 2016;  
256 Liu et al., 2023; Shen et al., 2017; Huang et al., 2016; Choi et al., 2020; Liu et al.,  
257 2018; Shu et al., 2023). MMAH<sup>+</sup>, as the dominant aminium species in most of cities,  
258 showed the highest ( $18.33 \pm 12.82 \text{ ng m}^{-3}$ ) and lowest ( $1.07 \pm 0.55 \text{ ng m}^{-3}$ ) average  
259 concentrations in HEB and WLMQ, respectively. DEAH<sup>+</sup> was the most abundant  
260 aminium species in TY and GZ, with average concentrations of  $22.62 \pm 17.62 \text{ ng m}^{-3}$   
261 and  $8.16 \pm 4.65 \text{ ng m}^{-3}$ , respectively (**Tables S1** and **S3**). Two previous studies  
262 conducted in the GZ area in winter (2021 and 2015–2016) showed similar average  
263 DEAH<sup>+</sup> ( $\sim 7 \text{ ng m}^{-3}$ ) levels to this study (Liu et al., 2022b; Shu et al., 2023). However,  
264 DEAH<sup>+</sup> was not identified as the dominant aminium component in these two previous  
265 studies. Furthermore, lower aminium concentrations ( $< 8 \text{ ng m}^{-3}$ ) were generally  
266 found in most of the marine and polar regions (Dall’osto et al., 2019; Corral et al.,



267 2022). In general, the concentration and composition of aminiums vary spatially,  
268 which may be attributed to spatial differences in amine sources, emission intensities,  
269 and the main factors affecting aminium formation.

270 The average concentrations of TA in all the investigated cities exhibited a similar  
271 variation pattern from clean to polluted days, which was characterized by higher  
272 levels on polluted days (**Figure 2**). Specifically, the average aminium concentration  
273 showed an increase of up to 206% in HEB during the polluted period. TA  
274 concentrations in LZ, TY, CD, HZ, and GZ also increased greatly by 91% (in GZ)  
275 –190% (in TY). It seems that PM<sub>2.5</sub> pollution can be accompanied by an outbreak of  
276 aminiums. In contrast, a relatively small percentage increase in TA concentration  
277 during the polluted days was found in WH (57%), XA (50%), and BJ (25%). To  
278 further explore the linkage between changes in PM<sub>2.5</sub> and fluctuations in aminiums,  
279 the temporal variations in the mass concentrations of aminiums and PM<sub>2.5</sub> were  
280 compared across various cities (**Figure 3**). The concentrations of total and major  
281 aminiums in LZ, TY, HEB, WLMQ, CD, WH, HZ, GZ, and GY showed a temporal  
282 variation highly similar to that of PM<sub>2.5</sub>, as indicated by a significant correlation  
283 between TA and PM<sub>2.5</sub> in these cities ( $r = 0.61\text{--}0.85$ ,  $P < 0.05$ ). However, high levels  
284 of PM<sub>2.5</sub> can correspond to low levels of aminiums in XA (e.g., Dec. 29 and Jan. 2,  
285 14, 15, and 16) and BJ (e.g., Dec. 28, 30). The correlations between TA and PM<sub>2.5</sub> in  
286 these two cities were also insignificant ( $P > 0.05$ ). These results suggest that the  
287 formation of aminiums in XA and BJ during the polluted period may be constrained  
288 by some special factors, which will be revealed in the following discussion.





289

290 **Figure 3.** Temporal variations in the mass concentrations of aminiums and PM<sub>2.5</sub>

291 observed at the (a) LZ, (b) TY, (c) HEB, (d) BJ, (e) XA, (f) WLMQ, (g) CD, (h) WH,

292 (i) HZ, (j) GZ, and (k) GY sites.

293

294 **3.3. Formation of aminiums and potential ammonia suppression in aminium**

295 **outbreaks**

296 It is well documented that aminiums in PM<sub>2.5</sub> can be formed mainly via the

297 uptake of their gaseous form (i.e., amines) by aqueous particles, followed by

298 acid–base neutralization reactions (Ge et al., 2011b; Xie et al., 2018; Sauerwein and

299 Chan, 2017; Qiu and Zhang, 2013; Liu et al., 2023). To explore the formation of

300 particle aminiums at these investigated sites, the potential origins of the corresponding

301 gas-phase amines (as precursors of aminiums) were roughly analyzed (**Figure 4** and

302 **Figure S2**). We found that TA and major aminiums (e.g., MMAH<sup>+</sup>, DMAH<sup>+</sup>, and



303 DEAH<sup>+</sup>) showed a significant positive correlation ( $P < 0.05$ ) with either SO<sub>2</sub>, NO<sub>2</sub>, or  
304 K<sup>+</sup> (as indicators of fuel combustion and biomass burning (Tian et al., 2020; Liu et al.,  
305 2023; Kunwar and Kawamura, 2014)) in most of cities (**Figure 4** and **Figure S2**). In  
306 contrast, the concentrations of TA in XA were insignificantly correlated ( $P > 0.05$ )  
307 with those of SO<sub>2</sub>, NO<sub>2</sub>, and K<sup>+</sup>. This indicates that fossil fuel combustion or biomass  
308 burning were important contributors to atmospheric amines in these investigated  
309 cities, except for XA, during winter. However, it should be pointed out that this does  
310 not imply that the contributions of fossil fuel combustion and biomass burning to  
311 amines in XA were insignificant. This is because the traditional method of identifying  
312 amine sources through correlation analysis (Berta et al., 2023; Liu et al., 2022b; Liu et  
313 al., 2022a; Huang et al., 2022; Corral et al., 2022) can also have significant  
314 uncertainties, as implied by the following two cases. First, the uptake of amines by  
315 aerosol particles might be constrained by low ALW concentration, weak particle  
316 acidity, or high ammonia levels (Liu et al., 2022b; Chen et al., 2022a; Ge et al.,  
317 2011b; Sauerwein and Chan, 2017; Chan and Chan, 2013; Wang et al., 2010). Second,  
318 amines might be largely decomposed by atmospheric oxidants (e.g., hydroxyl radical  
319 and ozone) (Nielsen et al., 2012; Qiu and Zhang, 2013). Thus, given the  
320 abovementioned uncertainty and the lack of sufficient indicators to trace the source of  
321 amines, the following discussion focuses on the main factors affecting the formation  
322 of aminiums in particles.

323

324



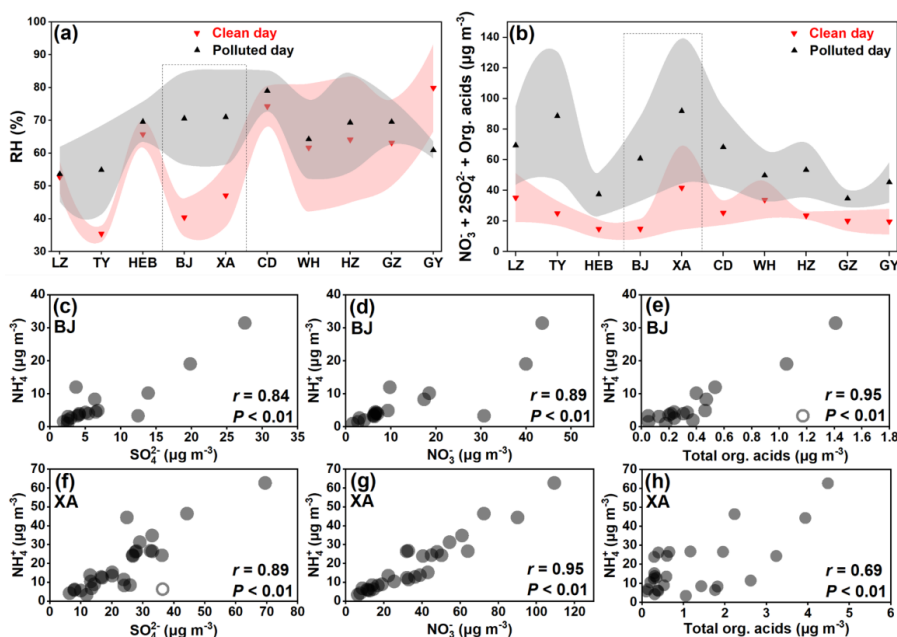


325  
 326 **Figure 4.** Diagrams presenting correlations between the concentrations of TA and  
 327 other parameters at (a–c) different sites. The colors of the different solid circles  
 328 indicate different correlation coefficients  $r$ . The size of the solid circle indicates the  
 329 significance of the correlation between the two corresponding parameters: the larger  
 330 circle indicates that the correlation is more significant, whereas the symbol “X”  
 331 indicates that the  $P$ -value is greater than 0.05.

332  
 333 The concentrations of TA in LZ, TY, HEB, WLMQ, CD, WH, HZ, GZ, and GY  
 334 showed significant positive correlations ( $P < 0.01$ ) with those of the acidic  
 335 components (e.g., NO<sub>3</sub><sup>-</sup>, SO<sub>4</sub><sup>2-</sup>, organic acids, and acidity (expressed as (NO<sub>3</sub><sup>-</sup> + 2SO<sub>4</sub><sup>2-</sup>  
 336 ) – NH<sub>4</sub><sup>+</sup>)), whereas an insignificant correlation ( $P > 0.05$ ) was found between them in  
 337 BJ and XA (**Figure 4** and **Figure S3**). Thus, acid-base chemistry was tightly  
 338 associated with the formation of aminiums in PM<sub>2.5</sub> at all sites excepting BJ and XA.  
 339 A recent laboratory study has suggested that amines can be neutralized by H<sub>3</sub>O<sup>+</sup> to  
 340 form aminiums within picoseconds under conditions of high concentrations of particle  
 341 sulfuric acid (Zhang et al., 2021). In addition, it has also been found that organic acids  
 342 (e.g., formic acid) are able to participate in the nucleation of methanesulfonic acid–  
 343 methylamine through an acid-base reaction (Zhang et al., 2022). The particles are  
 344 acidic (especially on polluted days) at all study sites, with an average pH value



345 ranging from 2.4 to 5.7 (**Tables S1–S3**). Amines can also partition into the particles  
346 by direct dissolution under high RH conditions (Ge et al., 2011b). Significantly  
347 increased RH values (i.e., high ALW) (**Figure 5a**) and acidic components (**Figure 5b**)  
348 on polluted days were also observed in XA and BJ. However, an insignificant ( $P >$   
349  $0.05$ ) correlation between aminiums and acidic components and ALW concentrations  
350 in XA and BJ, as well as a relatively small proportional increase in aminiums (**Figure**  
351 **2**) from clean to polluted days at these two sites suggested that the particle acidity and  
352 air RH may not be the dominant factors affecting aminium formation in XA and BJ.  
353 As we know, the oxidative degradation of amines is one of the main pathways for the  
354 removal of atmospheric amines (Qiu and Zhang, 2013; Murphy et al., 2007).  
355 Furthermore, for atmospheric oxidants (e.g., hydroxyl radical) reacting with low-  
356 molecular-weight alkylamines, a negative temperature dependence of the rate  
357 coefficients has been reported (Nielsen et al., 2012). However, the winter air  
358 temperature in northern China was relatively low ( $< 0$  °C in XA and BJ) (**Tables S1–**  
359 **S3**); moreover, there was no significant change in the atmospheric oxidation  
360 (indicated by  $O_x$  levels ( $O_x = O_3 + NO_2$ )) of polluted and clean days in XA and BJ. If  
361 atmospheric oxidation played a significant role in amine removal on polluted days in  
362 XA and BJ, it could lead to a decrease in the partitioning of amines into particles  
363 through acid-base neutralization reactions. Thus, atmospheric oxidation and  
364 temperature did not seem to be able to explain the increase in aminium concentrations  
365 in XA and BJ during the polluted days, as well as the insignificant correlation  
366 between aminiums and acidic components in XA and BJ.



367

368 **Figure 5.** The values of (a) RH and the concentrations of (b) acidic components

369 (expressed as  $\text{NO}_3^- + 2\text{SO}_4^{2-} + \text{total organic acids}$ ) on clean and polluted days in

370 different cities. The triangle and the shaded area represent the mean value and the

371 associated standard deviation, respectively. The correlations of  $\text{NH}_4^+$  with the

372 concentrations of  $\text{NO}_3^-$ ,  $\text{SO}_4^{2-}$ , and total organic acids at (c–e) BJ and (f–h) XA. Open

373 circles represent outliers.

374

375 Furthermore, we found that the concentrations of  $\text{NH}_4^+$  were strongly ( $P < 0.01$ )

376 correlated with those of acidic components in XA and BJ (**Figures 5c–h**). This

377 indicates that the acidity of the particles was sufficient for the uptake of ammonia to

378 form ammonium at these two study sites. Typically, the concentration of ammonia in

379 the atmosphere is 1 to 3 orders of magnitude higher than that of low-molecular-weight

380 alkylamines (Zheng et al., 2015; You et al., 2014; Yao et al., 2016; Wang et al., 2010).

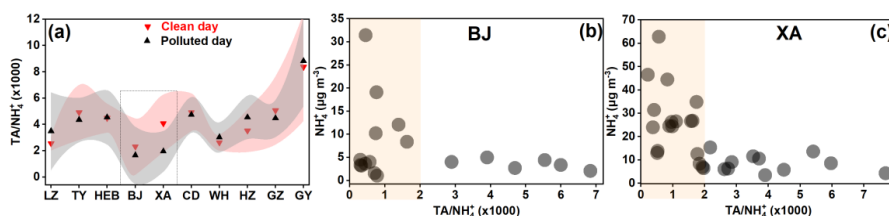


381 The uptake coefficient of alkylamines on acidic particles is lower than that of  
382 ammonia (Wang et al., 2010); moreover, Wang et al. (2010) proposed that fresh  
383 H<sub>2</sub>SO<sub>4</sub> particles can be overwhelmingly neutralized by ammonia when both amines  
384 and ammonia are present in the air. In particular, although the strong acidic condition  
385 was conducive to the formation of aminiums, amines and ammonia may compete for  
386 uptake into acidic aerosol particles (Chen et al., 2022a). Thus, the constraint of  
387 ammonia on amine uptake at much higher ammonia levels than amine levels may be a  
388 possible explanation for the insignificant acid-dependent aminium formation in XA  
389 and BJ (**Figures 4a,b**).

390 To further explore the role of ammonia (or ammonium) in aminium formation,  
391 the average ratios of TA to NH<sub>4</sub><sup>+</sup> on clean and polluted days in different cities were  
392 examined (**Figure 6a**). The average ratios of TA to NH<sub>4</sub><sup>+</sup> were found to be lowest in  
393 XA and BJ, especially on the polluted days, which was similar to the characteristics of  
394 the TA/(NH<sub>3</sub> + NH<sub>4</sub><sup>+</sup>) ratios (**Figure S4**). The sensitivity analysis of the TA/NH<sub>4</sub><sup>+</sup> ratio  
395 (the lowest in XA and BJ) to NH<sub>4</sub><sup>+</sup> changes (**Figures 6b,c** and **Figure S5**) suggests  
396 that when TA/NH<sub>4</sub><sup>+</sup> > 2, the NH<sub>4</sub><sup>+</sup> concentrations in XA and BJ remained at a relatively  
397 low level (less than 6 μg m<sup>-3</sup> and 15 μg m<sup>-3</sup> in BJ and XA, respectively) with the  
398 increase of TA/NH<sub>4</sub><sup>+</sup> ratio, indicating that the formation of aminiums was not limited  
399 by ammonia at low amine and ammonium levels (in this case, TA was significantly (*P*  
400 < 0.01) correlated with NH<sub>4</sub><sup>+</sup>). When TA/NH<sub>4</sub><sup>+</sup> < 2, the formation of aminiums may be  
401 constrained by higher amine and ammonium levels, which can also be supported by  
402 the insignificant (*P* > 0.05) correlation between TA and NH<sub>4</sub><sup>+</sup> in this case. In contrast,



403 the distributions of the ratios of TA to  $\text{NH}_4^+$  in other cities were in ranges greater than  
404 2 (**Figure S5**). The TA concentrations were thus significantly positively correlated  
405 with ammonium in these cities (excepting BJ and XA) (**Figure 4**). A recent study on  
406 the uptake of marine aerosol DMA by acidic aerosols has found that the  
407 concentrations of particle  $\text{DMAH}^+$  generally decreased with increasing atmospheric  
408 ammonia concentrations (Chen et al., 2022a); moreover, these researchers proposed  
409 the possibility that aminiums can be displaced by ammonia in a high ammonia  
410 environment. Accordingly, high atmospheric ammonia levels can indeed constrain the  
411 conversion of amines to aminiums, even if the aerosol is acidic. In addition, due to the  
412 lower VC values (**Tables S1–S3**) on polluted days compared to clean days, the  
413 atmospheric amines were less able to diffuse on polluted days. This may result in an  
414 accumulation of aminiums on polluted days via acid-base chemistry. However, the  
415 most significant decrease in  $\text{TA}/\text{NH}_4^+$  and  $\text{TA}/(\text{NH}_3 + \text{NH}_4^+)$  ratios from clean to  
416 polluted days occurred in XA, followed by BJ (**Figure 6a** and **Figure S4**). These  
417 results indicate that the extraction ratio of amines relative to ammonia on acidic  
418 particles was significantly reduced from clean to polluted days in XA and BJ.  
419 Presumably, the aminiums/ammonium ratio was likely an important indicator to  
420 reveal the competitive uptake of ammonia against amines on acidic aerosols, or the  
421 displacement of aminiums by ammonia in a high ammonia environment. Thus, this  
422 study provides a special field case that emphasizes the potential suppression of  
423 ammonia on aminium outbreaks during the polluted days.



424

425 **Figure 6.** The (a) average ratio of TA to NH<sub>4</sub><sup>+</sup> on clean and polluted days in different  
426 cities. The triangle and the shaded area represent the mean value and the associated  
427 standard deviation, respectively. Scatterplots of the mass concentrations of NH<sub>4</sub><sup>+</sup> with  
428 the ratio of TA to NH<sub>4</sub><sup>+</sup> at the (b) BJ and (c) XA sites.

429

#### 430 4. Conclusions and atmospheric implications

431 The concentrations, compositions, and temporal and spatial variations of  
432 aminiums in PM<sub>2.5</sub> in 11 different Chinese cities during the winter were systematically  
433 investigated. In particular, we focused on the differences in aminium concentration  
434 between polluted and clean days, as well as the key factors affecting the aminium  
435 outbreak during the polluted days. Specifically, MMAH<sup>+</sup> was the dominant species  
436 among the aminiums investigated in PM<sub>2.5</sub> in most cities, including LZ, XA, HEB,  
437 BJ, WLMQ, HZ, WH, CD, and GY, followed by DMAH<sup>+</sup>. In contrast, DEAH<sup>+</sup> was  
438 found to be the most abundant aminium species in TY and GZ, followed by MMAH<sup>+</sup>  
439 and DMAH<sup>+</sup>. This result can be attributed to the fact that the main sources of amines  
440 in TY and GZ were significantly different from those in other cities. However, due to  
441 the lack of amine emission inventories and sufficient tracers in these investigated  
442 cities, this study did not provide a detailed analysis of the specific sources of amines  
443 in these investigated cities.

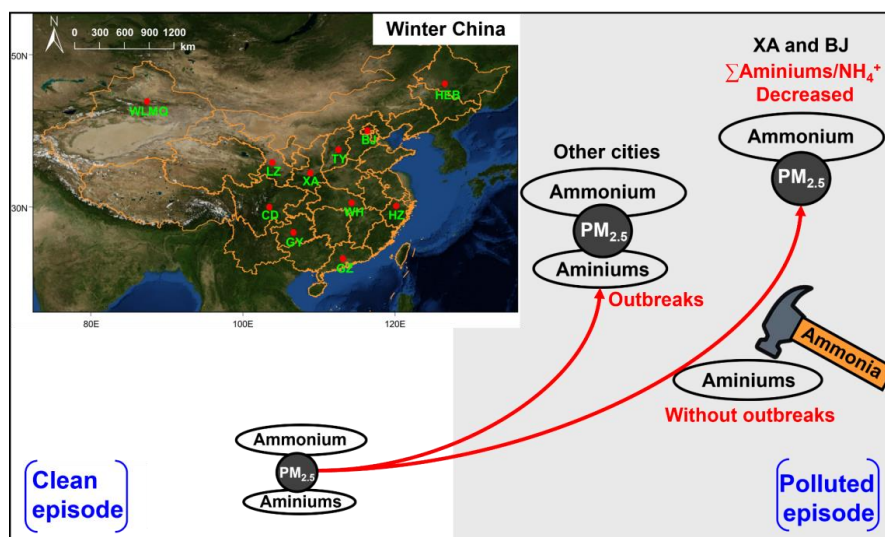


444 We found that the concentrations of TA and major aminiums in all cities showed  
445 a similar pattern of variation from the clean days to the polluted days, which was  
446 characterized by higher levels on the polluted days. However, the lowest percentage  
447 increase in TA concentration during the polluted days was found in XA (50%) and BJ  
448 (25%). Moreover, the concentrations of TA in XA and BJ were insignificantly ( $P >$   
449  $0.05$ ) correlated with those of  $PM_{2.5}$  and the main acidic components in  $PM_{2.5}$ .  
450 However, the significant correlations of TA with  $PM_{2.5}$  and the main acidic  
451 components were observed in other cities. Thus, acid-base chemistry was strongly  
452 associated with the formation of aminiums in  $PM_{2.5}$  in all cities with the exception of  
453 XA and BJ. The concentrations of  $NH_4^+$  were significantly ( $P < 0.01$ ) correlated with  
454 those of the acidic components in XA and BJ, indicating that the acidity of the  
455 particles was sufficient for the uptake of ammonia to form ammonium at these two  
456 sites. Further, based on the sensitivity analysis of the TA/ $NH_4^+$  ratio (the lowest in XA  
457 and BJ) to  $NH_4^+$  changes as well as excluding the effects of ALW and atmospheric  
458 oxidation, we proposed a possibility about the competitive uptake of ammonia against  
459 amines on acidic aerosols in the ambient atmosphere in XA and BJ. This  
460 consideration may explain the insignificant acid-dependent aminium formation in XA  
461 and BJ. The main finding of this study has been illustrated in a diagram (**Figure 7**).

462 In general, this study has preliminarily explored the characteristics of aminiums,  
463 ammonium, and  $PM_{2.5}$  from the clean days to the polluted days according to the  
464 observational data from 11 different Chinese cities, highlighting the possibility of the  
465 competitive uptake of ammonia versus amines on acidic aerosols, or the displacement



466 of aminiums by ammonia under a high ammonia condition. Although a recent study  
 467 has also demonstrated that the possibility of individual aminium was displaced by  
 468 ammonia in an environment of high ammonia level (Chen et al., 2022a), the uptake of  
 469 amines on particles to form aminiums and the relevant influencing factors are still not  
 470 fully understood in terms of mechanism. This is because acidity, environmental  
 471 ammonia and amine content, temperature, and liquid-phase reactions all affect the  
 472 uptake of amines, although acid-base neutralization of amines seems to be the most  
 473 important pathway for amine uptake. Furthermore, if the uptake of amines is  
 474 significantly constrained by the aforementioned factors, the traditional source  
 475 apportionment methods using correlation analysis between particle aminiums and  
 476 tracers will have significant uncertainty due to inefficient partitioning of the source  
 477 amine into the particle phase.



478  
 479 **Figure 7.** Conceptual illustration showing the characteristics of aminiums,  
 480 ammonium, and PM<sub>2.5</sub> from the clean days to the polluted days. The map was





481 obtained from <sup>©</sup>MeteoInfoMap (version 3.3.0) (Chinese Academy of Meteorological  
482 Sciences, China).

483

484 **Data availability.** The data in this study are available at  
485 <https://doi.org/10.5281/zenodo.11102019> (Xu et al., 2024).

486

487 **Conflict of interest.** The authors declare no conflicts of interest relevant to this study.

488

489 **Supplement.** Four tables (Tables S1–S4) and five extensive figures (Figures S1–S5).

490

491 **Author contributions.** YX and HYX designed the study. YX, YJM, QBS, HWX, and  
492 HX performed field measurements and sample collection; TL performed chemical  
493 analysis; YX performed data analysis; YX wrote the original manuscript; and YX  
494 reviewed and edited the manuscript.

495

496 **Financial support.** This study was kindly supported by the National Natural Science  
497 Foundation of China through grant 42303081 (Y. Xu) and Shanghai “Science and  
498 Technology Innovation Action Plan” Shanghai Sailing Program through grant  
499 22YF1418700 (Y. Xu).

500

## 501 **References**

502 Berta, V. Z., Russell, L. M., Price, D. J., Chen, C. L., Lee, A. K. Y., Quinn, P. K.,



503 Bates, T. S., Bell, T. G., and Behrenfeld, M. J.: Non-volatile marine and non-  
504 refractory continental sources of particle-phase amine during the North Atlantic  
505 Aerosols and Marine Ecosystems Study (NAAMES), *Atmos. Chem. Phys.*, 23, 2765-  
506 2787, 10.5194/acp-23-2765-2023, 2023.

507 Chan, L. P. and Chan, C. K.: Role of the Aerosol Phase State in  
508 Ammonia/Amines Exchange Reactions, *Environmental Science & Technology*, 47,  
509 5755-5762, 10.1021/es4004685, 2013.

510 Chang, Y., Wang, H., Gao, Y., Jing, S. a., Lu, Y., Lou, S., Kuang, Y., Cheng, K.,  
511 Ling, Q., Zhu, L., Tan, W., and Huang, R.-J.: Nonagricultural Emissions Dominate  
512 Urban Atmospheric Amines as Revealed by Mobile Measurements, *Geophysical*  
513 *Research Letters*, 49, e2021GL097640, <https://doi.org/10.1029/2021GL097640>, 2022.

514 Chen, D., Yao, X., Chan, C. K., Tian, X., Chu, Y., Clegg, S. L., Shen, Y., Gao, Y.,  
515 and Gao, H.: Competitive Uptake of Dimethylamine and Trimethylamine against  
516 Ammonia on Acidic Particles in Marine Atmospheres, *Environmental Science &*  
517 *Technology*, 56, 5430-5439, 10.1021/acs.est.1c08713, 2022a.

518 Chen, Y., Lin, Q., Li, G., and An, T.: A new method of simultaneous  
519 determination of atmospheric amines in gaseous and particulate phases by gas  
520 chromatography-mass spectrometry, *Journal of Environmental Sciences*, 114, 401-  
521 411, <https://doi.org/10.1016/j.jes.2021.09.027>, 2022b.

522 Chen, Y., Tian, M., Huang, R. J., Shi, G., Wang, H., Peng, C., Cao, J., Wang, Q.,  
523 Zhang, S., Guo, D., Zhang, L., and Yang, F.: Characterization of urban amine-  
524 containing particles in southwestern China: seasonal variation, source, and processing,



- 525 Atmos. Chem. Phys., 19, 3245-3255, 10.5194/acp-19-3245-2019, 2019.
- 526 Choi, N. R., Lee, J. Y., Ahn, Y. G., and Kim, Y. P.: Determination of atmospheric  
527 amines at Seoul, South Korea via gas chromatography/tandem mass spectrometry,  
528 Chemosphere, 258, 127367, 10.1016/j.chemosphere.2020.127367, 2020.
- 529 Corral, A. F., Choi, Y., Collister, B. L., Crosbie, E., Dadashazar, H., DiGangi, J.  
530 P., Diskin, G. S., Fenn, M., Kirschler, S., Moore, R. H., Nowak, J. B., Shook, M. A.,  
531 Stahl, C. T., Shingler, T., Thornhill, K. L., Voigt, C., Ziemba, L. D., and Sorooshian,  
532 A.: Dimethylamine in cloud water: a case study over the northwest Atlantic Ocean,  
533 Environmental Science: Atmospheres, 2, 1534-1550, 10.1039/D2EA00117A, 2022.
- 534 Dall'Osto, M., Airs, R. L., Beale, R., Cree, C., Fitzsimons, M. F., Beddows, D.,  
535 Harrison, R. M., Ceburnis, D., O'Dowd, C., Rinaldi, M., Paglione, M., Nenes, A.,  
536 Decesari, S., and Simó, R.: Simultaneous Detection of Alkylamines in the Surface  
537 Ocean and Atmosphere of the Antarctic Sympagic Environment, ACS Earth and  
538 Space Chemistry, 3, 854-862, 10.1021/acsearthspacechem.9b00028, 2019.
- 539 Facchini, M. C., Decesari, S., Rinaldi, M., Carbone, C., Finessi, E., Mircea, M.,  
540 Fuzzi, S., Moretti, F., Tagliavini, E., Ceburnis, D., and O'Dowd, C. D.: Important  
541 Source of Marine Secondary Organic Aerosol from Biogenic Amines, Environmental  
542 Science & Technology, 42, 9116-9121, 10.1021/es8018385, 2008.
- 543 Feng, X., Wang, C., Feng, Y., Cai, J., Zhang, Y., Qi, X., Li, Q., Li, J., and Chen,  
544 Y.: Outbreaks of Ethyl-Amines during Haze Episodes in North China Plain: A  
545 Potential Source of Amines from Ethanol Gasoline Vehicle Emission, Environmental  
546 Science & Technology Letters, 9, 306-311, 10.1021/acs.estlett.2c00145, 2022.



547 Gani, S., Bhandari, S., Seraj, S., Wang, D. S., Patel, K., Soni, P., Arub, Z., Habib,  
548 G., Hildebrandt Ruiz, L., and Apte, J. S.: Submicron aerosol composition in the  
549 world's most polluted megacity: the Delhi Aerosol Supersite study, *Atmos. Chem.*  
550 *Phys.*, 19, 6843-6859, 10.5194/acp-19-6843-2019, 2019.

551 Ge, X., Wexler, A. S., and Clegg, S. L.: Atmospheric amines – Part I. A review,  
552 *Atmospheric Environment*, 45, 524-546,  
553 <https://doi.org/10.1016/j.atmosenv.2010.10.012>, 2011a.

554 Ge, X., Wexler, A. S., and Clegg, S. L.: Atmospheric amines – Part II.  
555 Thermodynamic properties and gas/particle partitioning, *Atmospheric Environment*,  
556 45, 561-577, <https://doi.org/10.1016/j.atmosenv.2010.10.013>, 2011b.

557 Gibb, S. W., Mantoura, R. F. C., and Liss, P. S.: Ocean-atmosphere exchange and  
558 atmospheric speciation of ammonia and methylamines in the region of the NW  
559 Arabian Sea, *Global Biogeochemical Cycles*, 13, 161-178,  
560 <https://doi.org/10.1029/98GB00743>, 1999.

561 Ho, K.-F., Ho, S. S. H., Huang, R.-J., Chuang, H.-C., Cao, J.-J., Han, Y., Lui, K.-  
562 H., Ning, Z., Chuang, K.-J., Cheng, T.-J., Lee, S.-C., Hu, D., Wang, B., and Zhang,  
563 R.: Chemical composition and bioreactivity of PM<sub>2.5</sub> during 2013 haze events in  
564 China, *Atmospheric Environment*, 126, 162-170,  
565 <https://doi.org/10.1016/j.atmosenv.2015.11.055>, 2016.

566 Ho, K. F., Ho, S. S. H., Huang, R.-J., Liu, S. X., Cao, J.-J., Zhang, T., Chuang,  
567 H.-C., Chan, C. S., Hu, D., and Tian, L.: Characteristics of water-soluble organic  
568 nitrogen in fine particulate matter in the continental area of China, *Atmospheric*



- 569 Environment, 106, 252-261, <https://doi.org/10.1016/j.atmosenv.2015.02.010>, 2015.
- 570 Huang, S., Song, Q., Hu, W., Yuan, B., Liu, J., Jiang, B., Li, W., Wu, C., Jiang,  
571 F., Chen, W., Wang, X., and Shao, M.: Chemical composition and sources of amines  
572 in PM<sub>2.5</sub> in an urban site of PRD, China, Environmental Research, 212, 113261,  
573 <https://doi.org/10.1016/j.envres.2022.113261>, 2022.
- 574 Huang, X., Deng, C., Zhuang, G., Lin, J., and Xiao, M.: Quantitative analysis of  
575 aliphatic amines in urban aerosols based on online derivatization and high  
576 performance liquid chromatography, Environmental Science: Processes & Impacts,  
577 18, 796-801, 10.1039/C6EM00197A, 2016.
- 578 Kunwar, B. and Kawamura, K.: One-year observations of carbonaceous and  
579 nitrogenous components and major ions in the aerosols from subtropical Okinawa  
580 Island, an outflow region of Asian dusts, Atmos. Chem. Phys., 14, 1819-1836.  
581 <https://doi.org/10.5194/acp-14-1819-2014>, 2014.
- 582 Li, G., Liao, Y., Hu, J., Lu, L., Zhang, Y., Li, B., and An, T.: Activation of NF- $\kappa$ B  
583 pathways mediating the inflammation and pulmonary diseases associated with  
584 atmospheric methylamine exposure, Environmental pollution, 252, 1216-1224,  
585 <https://doi.org/10.1016/j.envpol.2019.06.059>, 2019.
- 586 Lin, X., Xu, Y., Zhu, R.-G., Xiao, H.-W., and Xiao, H.-Y.: Proteinaceous Matter  
587 in PM<sub>2.5</sub> in Suburban Guiyang, Southwestern China: Decreased Importance in Long-  
588 Range Transport and Atmospheric Degradation, J. Geophys. Res.: Atmos., 128,  
589 e2023JD038516, <https://doi.org/10.1029/2023JD038516>, 2023.
- 590 Liu, C., Li, H., Zheng, H., Wang, G., Qin, X., Chen, J., Zhou, S., Lu, D., Liang,



591 G., Song, X., Duan, Y., Liu, J., Huang, K., and Deng, C.: Ocean Emission Pathway  
592 and Secondary Formation Mechanism of Aminiums Over the Chinese Marginal Sea,  
593 Journal of Geophysical Research: Atmospheres, 127, e2022JD037805,  
594 <https://doi.org/10.1029/2022JD037805>, 2022a.

595 Liu, F., Bi, X., Zhang, G., Peng, L., Lian, X., Lu, H., Fu, Y., Wang, X., Peng, P.  
596 a., and Sheng, G.: Concentration, size distribution and dry deposition of amines in  
597 atmospheric particles of urban Guangzhou, China, Atmospheric Environment, 171,  
598 279-288, <https://doi.org/10.1016/j.atmosenv.2017.10.016>, 2017.

599 Liu, F., Zhang, G., Lian, X., Fu, Y., Lin, Q., Yang, Y., Bi, X., Wang, X., Peng, P.  
600 a., and Sheng, G.: Influence of meteorological parameters and oxidizing capacity on  
601 characteristics of airborne particulate amines in an urban area of the Pearl River Delta,  
602 China, Environmental Research, 212, 113212,  
603 <https://doi.org/10.1016/j.envres.2022.113212>, 2022b.

604 Liu, F., Bi, X., Zhang, G., Lian, X., Fu, Y., Yang, Y., Lin, Q., Jiang, F., Wang, X.,  
605 Peng, P. a., and Sheng, G.: Gas-to-particle partitioning of atmospheric amines  
606 observed at a mountain site in southern China, Atmospheric Environment, 195, 1-11,  
607 <https://doi.org/10.1016/j.atmosenv.2018.09.038>, 2018.

608 Liu, T., Xu, Y., Sun, Q.-B., Xiao, H.-W., Zhu, R.-G., Li, C.-X., Li, Z.-Y., Zhang,  
609 K.-Q., Sun, C.-X., and Xiao, H.-Y.: Characteristics, Origins, and Atmospheric  
610 Processes of Amines in Fine Aerosol Particles in Winter in China, J. Geophys. Res.:  
611 Atmos., 128, e2023JD038974, <https://doi.org/10.1029/2023JD038974>, 2023.

612 Liu, Z., Li, M., Wang, X., Liang, Y., Jiang, Y., Chen, J., Mu, J., Zhu, Y., Meng,



613 H., Yang, L., Hou, K., Wang, Y., and Xue, L.: Large contributions of anthropogenic  
614 sources to amines in fine particles at a coastal area in northern China in winter,  
615 Science of The Total Environment, 839, 156281,  
616 <https://doi.org/10.1016/j.scitotenv.2022.156281>, 2022c.

617 Ma, Y. J., Xu, Y., Yang, T., Xiao, H. W., and Xiao, H. Y.: Measurement report:  
618 Characteristics of nitrogen-containing organics in PM<sub>2.5</sub> in Urumqi, northwest China:  
619 differential impacts of combustion of fresh and old-age biomass materials,  
620 EGU sphere, 2024, 1-48, 10.5194/egusphere-2023-2514, 2024.

621 Møller, K. H., Berndt, T., and Kjaergaard, H. G.: Atmospheric Autoxidation of  
622 Amines, Environmental Science & Technology, 54, 11087-11099,  
623 10.1021/acs.est.0c03937, 2020.

624 Murphy, S. M., Sorooshian, A., Kroll, J. H., Ng, N. L., Chhabra, P., Tong, C.,  
625 Surratt, J. D., Knipping, E., Flagan, R. C., and Seinfeld, J. H.: Secondary aerosol  
626 formation from atmospheric reactions of aliphatic amines, Atmos. Chem. Phys., 7,  
627 2313-2337, 10.5194/acp-7-2313-2007, 2007.

628 Nielsen, C. J., Herrmann, H., and Weller, C.: Atmospheric chemistry and  
629 environmental impact of the use of amines in carbon capture and storage (CCS),  
630 Chemical Society Reviews, 41, 6684-6704, 10.1039/C2CS35059A, 2012.

631 Qiu, C. and Zhang, R.: Multiphase chemistry of atmospheric amines, Physical  
632 Chemistry Chemical Physics, 15, 5738-5752, 10.1039/C3CP43446J, 2013.

633 Sauerwein, M. and Chan, C. K.: Heterogeneous uptake of ammonia and  
634 dimethylamine into sulfuric and oxalic acid particles, Atmos. Chem. Phys., 17, 6323-



635 6339, 10.5194/acp-17-6323-2017, 2017.

636 Shen, W., Ren, L., Zhao, Y., Zhou, L., Dai, L., Ge, X., Kong, S., Yan, Q., Xu, H.,

637 Jiang, Y., He, J., Chen, M., and Yu, H.: C1-C2 alkyl aminiums in urban aerosols:

638 Insights from ambient and fuel combustion emission measurements in the Yangtze

639 River Delta region of China, *Environmental pollution*, 230, 12-21,

640 <https://doi.org/10.1016/j.envpol.2017.06.034>, 2017.

641 Shen, X., Chen, J., Li, G., and An, T.: A new advance in the pollution profile,

642 transformation process, and contribution to aerosol formation and aging of

643 atmospheric amines, *Environmental Science: Atmospheres*, 3, 444-473,

644 10.1039/D2EA00167E, 2023.

645 Shu, Q., Pei, C., Lin, X., Hong, D., Lai, S., and Zhang, Y.: Variations of

646 aminiums in fine particles at a suburban site in Guangzhou, China: Importance of

647 anthropogenic and natural emissions, *Particuology*, 80, 140-147,

648 <https://doi.org/10.1016/j.partic.2022.11.019>, 2023.

649 Tao, Y., Liu, T., Yang, X., and Murphy, J. G.: Kinetics and Products of the

650 Aqueous Phase Oxidation of Triethylamine by OH, *ACS Earth and Space Chemistry*,

651 5, 1889-1895, 10.1021/acsearthspacechem.1c00162, 2021.

652 Tao, Y., Ye, X., Jiang, S., Yang, X., Chen, J., Xie, Y., and Wang, R.: Effects of

653 amines on particle growth observed in new particle formation events, *Journal of*

654 *Geophysical Research: Atmospheres*, 121, 324-335,

655 <https://doi.org/10.1002/2015JD024245>, 2016.

656 Tian, D., Fan, J., Jin, H., Mao, H., Geng, D., Hou, S., Zhang, P., and Zhang, Y.:





657 Characteristic and Spatiotemporal Variation of Air Pollution in Northern China Based  
658 on Correlation Analysis and Clustering Analysis of Five Air Pollutants, Journal of  
659 Geophysical Research: Atmospheres, 125, e2019JD031931,  
660 <https://doi.org/10.1029/2019JD031931>, 2020.

661 Tong, D., Chen, J., Qin, D., Ji, Y., Li, G., and An, T.: Mechanism of atmospheric  
662 organic amines reacted with ozone and implications for the formation of secondary  
663 organic aerosols, Science of The Total Environment, 737, 139830,  
664 <https://doi.org/10.1016/j.scitotenv.2020.139830>, 2020.

665 Wang, L., Lal, V., Khalizov, A. F., and Zhang, R.: Heterogeneous Chemistry of  
666 Alkylamines with Sulfuric Acid: Implications for Atmospheric Formation of  
667 Alkylammonium Sulfates, Environmental Science & Technology, 44, 2461-2465,  
668 [10.1021/es9036868](https://doi.org/10.1021/es9036868), 2010.

669 Wang, M., Wang, Q., Ho, S. S. H., Li, H., Zhang, R., Ran, W., Qu, L., Lee, S.-c.,  
670 and Cao, J.: Chemical characteristics and sources of nitrogen-containing organic  
671 compounds at a regional site in the North China Plain during the transition period of  
672 autumn and winter, Science of The Total Environment, 812, 151451,  
673 <https://doi.org/10.1016/j.scitotenv.2021.151451>, 2022.

674 Xie, H., Feng, L., Hu, Q., Zhu, Y., Gao, H., Gao, Y., and Yao, X.: Concentration  
675 and size distribution of water-extracted dimethylammonium and trimethylammonium in  
676 atmospheric particles during nine campaigns - Implications for sources, phase states  
677 and formation pathways, Science of The Total Environment, 631-632, 130-141,  
678 <https://doi.org/10.1016/j.scitotenv.2018.02.303>, 2018.



679 Xu, Y., Dong, X.-N., Xiao, H.-Y., He, C., and Wu, D.-S.: Water-Insoluble  
680 Components in Rainwater in Suburban Guiyang, Southwestern China: A Potential  
681 Contributor to Dissolved Organic Carbon, *Journal of Geophysical Research:*  
682 *Atmospheres*, 127, e2022JD037721, <https://doi.org/10.1029/2022JD037721>, 2022a.

683 Xu, Y., Dong, X.-N., Xiao, H.-Y., Zhou, J.-X., and Wu, D.-S.: Proteinaceous  
684 Matter and Liquid Water in Fine Aerosols in Nanchang, Eastern China: Seasonal  
685 Variations, Sources, and Potential Connections, *J. Geophys. Res.: Atmos.*, 127,  
686 e2022JD036589. <https://doi.org/10.1029/2022JD036589>, 2022b.

687 Xu, Y., Dong, X. N., He, C., Wu, D. S., Xiao, H. W., and Xiao, H. Y.: Mist  
688 cannon trucks can exacerbate the formation of water-soluble organic aerosol and  
689 PM<sub>2.5</sub> pollution in the road environment, *Atmos. Chem. Phys.*, 23, 6775-6788,  
690 10.5194/acp-23-6775-2023, 2023.

691 Xu, Y., Miyazaki, Y., Tachibana, E., Sato, K., Ramasamy, S., Mochizuki, T.,  
692 Sadanaga, Y., Nakashima, Y., Sakamoto, Y., Matsuda, K., and Kajii, Y.: Aerosol  
693 Liquid Water Promotes the Formation of Water-Soluble Organic Nitrogen in  
694 Submicrometer Aerosols in a Suburban Forest, *Environ. Sci. Technol.*, 54, 1406-1414.  
695 <https://doi.org/10.1021/acs.est.1409b05849>, 2020.

696 Xu, Y., Liu, T., Ma, Y. J., Sun, Q. B., Xiao, H. W., Xiao, H., and Xiao, H. Y.:  
697 Characteristics of aminiums in PM<sub>2.5</sub> during winter clean and polluted episodes in  
698 China: aminium outbreak and its constraint, Zenodo [data set],  
699 <https://doi.org/10.5281/zenodo.11102019>, 2024.

700 Yang, T., Xu, Y., Ye, Q., Ma, Y. J., Wang, Y. C., Yu, J. Z., Duan, Y. S., Li, C. X.,



701 Xiao, H. W., Li, Z. Y., Zhao, Y., and Xiao, H. Y.: Spatial and diurnal variations of  
702 aerosol organosulfates in summertime Shanghai, China: potential influence of  
703 photochemical processes and anthropogenic sulfate pollution, *Atmos. Chem. Phys.*,  
704 23, 13433-13450, 10.5194/acp-23-13433-2023, 2023a.

705 Yang, X.-Y., Cao, F., Fan, M.-Y., Lin, Y.-C., Xie, F., and Zhang, Y.-L.: Seasonal  
706 variations of low molecular alkyl amines in PM<sub>2.5</sub> in a North China Plain industrial  
707 city: Importance of secondary formation and combustion emissions, *Science of The*  
708 *Total Environment*, 857, 159371, <https://doi.org/10.1016/j.scitotenv.2022.159371>,  
709 2023b.

710 Yao, L., Wang, M. Y., Wang, X. K., Liu, Y. J., Chen, H. F., Zheng, J., Nie, W.,  
711 Ding, A. J., Geng, F. H., Wang, D. F., Chen, J. M., Worsnop, D. R., and Wang, L.:  
712 Detection of atmospheric gaseous amines and amides by a high-resolution time-of-  
713 flight chemical ionization mass spectrometer with protonated ethanol reagent ions,  
714 *Atmos. Chem. Phys.*, 16, 14527-14543, 10.5194/acp-16-14527-2016, 2016.

715 Yao, L., Garmash, O., Bianchi, F., Zheng, J., Yan, C., Kontkanen, J., Junninen,  
716 H., Mazon, S. B., Ehn, M., Paasonen, P., Sipilä, M., Wang, M., Wang, X., Xiao, S.,  
717 Chen, H., Lu, Y., Zhang, B., Wang, D., Fu, Q., Geng, F., Li, L., Wang, H., Qiao, L.,  
718 Yang, X., Chen, J., Kerminen, V.-M., Petäjä, T., Worsnop, D. R., Kulmala, M., and  
719 Wang, L.: Atmospheric new particle formation from sulfuric acid and amines in a  
720 Chinese megacity, *Science*, 361, 278-281, doi:10.1126/science.aao4839, 2018.

721 You, Y., Kanawade, V. P., de Gouw, J. A., Guenther, A. B., Madronich, S., Sierra-  
722 Hernández, M. R., Lawler, M., Smith, J. N., Takahama, S., Ruggeri, G., Koss, A.,



723 Olson, K., Baumann, K., Weber, R. J., Nenes, A., Guo, H., Edgerton, E. S., Porcelli,  
724 L., Brune, W. H., Goldstein, A. H., and Lee, S. H.: Atmospheric amines and ammonia  
725 measured with a chemical ionization mass spectrometer (CIMS), *Atmos. Chem.*  
726 *Phys.*, 14, 12181-12194, 10.5194/acp-14-12181-2014, 2014.

727 Zhang, R., Shen, J., Xie, H. B., Chen, J., and Elm, J.: The role of organic acids in  
728 new particle formation from methanesulfonic acid and methylamine, *Atmos. Chem.*  
729 *Phys.*, 22, 2639-2650, 10.5194/acp-22-2639-2022, 2022.

730 Zhang, W., Zhong, J., Shi, Q., Gao, L., Ji, Y., Li, G., An, T., and Francisco, J. S.:  
731 Mechanism for Rapid Conversion of Amines to Ammonium Salts at the Air-Particle  
732 Interface, *Journal of the American Chemical Society*, 143, 1171-1178,  
733 10.1021/jacs.0c12207, 2021.

734 Zhang, Y.-L. and Cao, F.: Fine particulate matter (PM<sub>2.5</sub>) in China at a city level,  
735 *Scientific Reports*, 5, 14884, 10.1038/srep14884, 2015.

736 Zheng, J., Ma, Y., Chen, M., Zhang, Q., Wang, L., Khalizov, A. F., Yao, L.,  
737 Wang, Z., Wang, X., and Chen, L.: Measurement of atmospheric amines and ammonia  
738 using the high resolution time-of-flight chemical ionization mass spectrometry,  
739 *Atmospheric Environment*, 102, 249-259,  
740 <https://doi.org/10.1016/j.atmosenv.2014.12.002>, 2015.

741